Compton Scattering:
A Theory and Experiments

Samir A Hamouda

Department of physics,
University of Benghazi, Libya

Abstract: *Introduction: Compton scattering is a technique for determining the momentum distribution of electrons in condensed matter. When monochromatic photons are Compton scattered (inelastically scattered) in a fixed direction, the observed energy spectrum of the scattered photons is Doppler-broadened due to the motion of the target electrons. The objective of this review is to present the Compton scattering theory to researchers generally unfamiliar with this phenomenon and to lead the researchers to understanding of the fundamental principles of the Compton Scattering Theory and of the way in which they are employed in logical deductions and analyses. In this review, the theoretical and experimental considerations and energy limitations of the Compton scattering method are discussed. The method for extracting information about ground-state electron momentum densities through an analysis of the Compton line shape is presented. The various Compton sources and Compton scattering in current use are reviewed. Since 1970 Compton profile measurements have become more frequent and the experimental results for many Z-elements reported in the literature have been quoted to an accuracy of better than 1% for the total profiles. Today the Compton scattering is acknowledged as an important technique for investing the electronic structure of materials; it provides a sensitive test for the accuracy of the resulting electron wave functions obtained from different theoretical models. This has been demonstrated in view of the Compton scattering experiments successfully performed over a wide range of incident photon energies (10 - 662 KeV) used in various Compton spectrometer systems distributed around the world.*

Keywords: Compton scattering, high energy gamma-ray spectroscopy, methods and technologies, characterization techniques, modeling and materials theory.

1. Introduction

following the discovery and explanation of the effect in 1923 by A. H. Compton [1,2]. It was then recognized that when monochromatic photons are Compton scattered (inelastically scattered) in a fixed direction, the observed energy spectrum of the scattered photons is Doppler-broadened due to the motion of the target electrons. A general review of the subject has been given by Cooper [3] and a detailed account is presented in a book edited by Williams [4]. DuMond [5] suggested that the Compton Effect would be a useful method for measuring the electronic momentum density of electronic systems. The link between the Compton scattering process and the electronic momentum density of the scattering system have motivated experimentalists as well as theoreticians to find interpretations for the Compton scattered spectrum. Unfortunately the development of Compton scattering method had to wait thirty years due to the experimental difficulties encountered as a result of the weakness of the Compton scattered radiation.

Renewed interest in the momentum density studies began in the mid 1960's as a result of the theoretical work by Platzman and Tzoar [6] and later by Eisenberger and Platzman [7]. This together with the availability of x-ray tubes with improved stability and greater power than those available to DuMond and his coworkers, helped in constructing apparatus coupled with crystal spectrometers that can provide both high intensity and high resolution. The initial experimental efforts of Cooper and Leake and Weiss [8], Cooper and Leake [9], Cooper and Williams [10], and Weiss and Phillips [11], have shown within the framework of the Impulse Approximation that Compton scattering offered a probe for measuring the electron momentum density of atoms, molecules and solids.

2. Materials and Methods

In the impulse approximation the differential cross-section in the nonrelativistic region is proportional to the Compton profile J (pz). The Compton profile J (pz) is defined as the projection of the ground state electron momentum density distribution, n (p), along the scattering vector (chosen as the pz axis) and is given by;

$$J(p_z) = \int\int n\,(p_x, p_y, p_z)\,dp_x\,dp_y \qquad (1)$$

The Compton profile given by equation (1) is of central importance because J (pz) represents the form in which results of experiments are presented. Furthermore, since J (pz) is directly related to the momentum density n (p), the Compton profile constitutes a sensitive test of the accuracy of different wave-function models.

When the incident photons are Compton scattered, the energy distribution of the scattered photons can be recorded and the double differential scattering cross-section $d^2\sigma/d\Omega d\omega$ obtained. The objective of this paper is to present the Compton scattering theory to researchers generally unfamiliar with this phenomenon and to lead the researchers to understanding of the fundamental principles of the Compton Scattering Theory and of the way in which they are employed in logical deductions and analyses. The main primary purpose of this paper is to show how the Compton profile J (p_z) given by equation (1) can be extracted from the measured double scattering cross-section, following the explanation of the Compton effect and the consequent development of the Compton scattering theory which have led to an interpretation of the experimental results in terms of the electronic wave functions of the scattering system.

The Compton Effect: The Compton Effect refers to the inelastic scattering of a photon by free electron initially at rest. A comprehensive historical development of this effect is presented by Stewart [12]. Compton [1] found that when a monochromatic x-ray is scattered by matter, it is separated into two distinct parts, one of the same wavelength as the primary beam and the other of increased wavelength. Compton called these the unmodified and the modified ray respectively. The wave-length of the unmodified ray is in accord with Thomson's classical theory of scattering x-rays [13] and the wave-length of the modified ray was explained by quantum theory.

Compton measured the amount of the shift and produced a theory which explained the experiments perfectly. He assumed that the incident radiation consisted of photons which had momentum as well as energy and treated the collision of a photon of energy $\hbar\omega$ and momentum $\hbar k$, colliding with a free electron initially at rest, as if he was dealing with a collision of ordinary material particles. The electron will recoil in order to satisfy simultaneously the laws of conservation of energy and momentum, and the photon will be scattered in some definite direction. The collision between the incident photon and a free stationary electron is shown in figure 1. Combining the laws of conservation of energy and momentum, Compton worked out the details of the collision and found the following relationship between shift in wavelength of the photon and scattering angle θ which exactly agreed with experiments.

$$\lambda_2 - \lambda_1 = (h/mc)\,(1 - \cos\theta) \qquad (2)$$

Where λ_1 and λ_2 are the incident and the scattered photon wavelengths respectively, h is Planck's constant, m is the electron rest mass, and c is the velocity of light. Equation (2) is the well-known expression for the Compton shift, or the difference in wavelength between the incident and the scattered photons. The length $h/mc = 2.426 \times 10^{-12}$ m is called the Compton wavelength λc which is equal to the wavelength of a photon whose energy is just equal to the rest energy of the electron $mc^2 = 0.51$ MeV. Therefore, the Compton Effect is likely to be noticeable only for photons with wavelengths of the order of the Compton wavelength h/mc. In the long wavelength limit, $\lambda \gg h/mc$, the angular distribution of the scattered photons agrees with the Thomson's classical theory [13, 14].
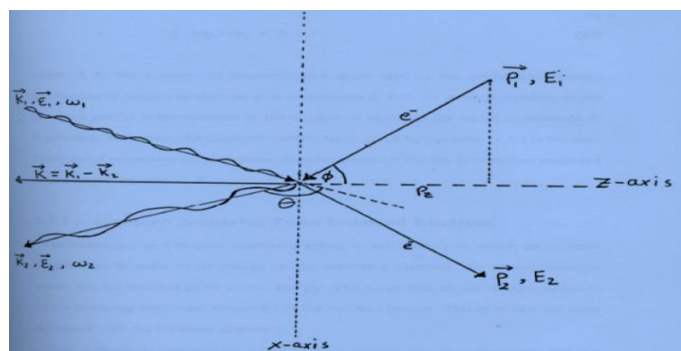

Figure 1: Schematic diagram describing the Compton scattering interaction between an incident photon with initial wave vector **K₁**, energy ω_1, unit polarization **ε₁** and an electron with initial momentum p_1 and energy E_1. The photon scatters at scattering angle θ with wave vector **K₂**, energy ω_2, unit polarization **ε₂** and the electron recoils with momentum **p₂** and energy **E₂.**

Rewriting equation (2) in terms of the incident ω_1 and scattered ω_2 photon energies, the Compton shift in energy becomes,

$$\omega_2 = \omega_1\,[1 + \omega_1/mc^2\,(1 - \cos\theta)]^{-1} \qquad (3)$$

This equation emphasizes the fact that the Compton shift in energy is very strongly dependent upon ω_1. At lower energy, photons are scattered with only moderate energy change, but at high energy, scattered photons suffer a very large change in energy. For incident energies of, say, 50 KeV and 400 KeV, both scattered at 45^0, the 50 KeV photons lose about 9% of their energy and the 400 KeV photons lose almost 44%.

Since the derivation of the Compton shift, equation (2), was based upon the assumptions that the struck electron is initially free and at rest, the nature of the scatterer, in fact does not enter into equation (2). As a result, the expression for the Compton shift, given by equation (2) does not provide any information about the target and the Compton theory appears at first a doubtful method for the study of the target electron. However, in a real target electrons are not free and stationary but bound and moving. In fact, the outer-shell electrons in atoms have velocities in the range $10^5 - 10^6$ ms^{-1} and the core electrons in heavy elements can attain relativistic velocities. Scattering of monochromatic radiation by electrons at rest should lead to a δ-function in Compton spectrum. However, it was subsequently found by Compton [2] that the Compton spectral line is broader than one would have expected from taking account of non-monochromaticity and of the angular divergence of the incident radiation (see figure2).
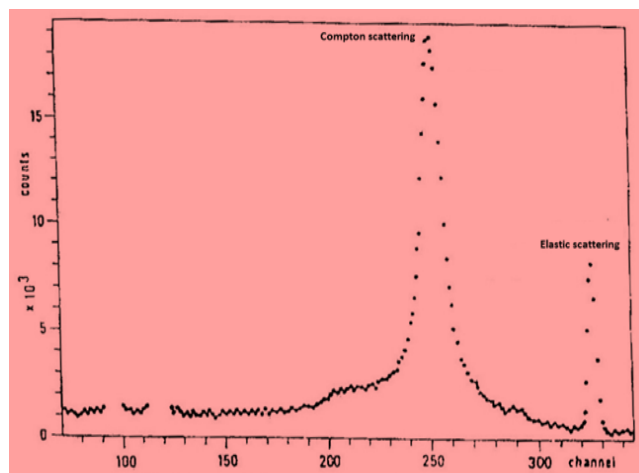

Figure 2: Shows the Elastic line and the Compton shifted line.

The development of Compton Scattering Theory.

Jauncy [15] was the first to show that the initial momentum of the scattering electrons play a part in the scattering process and influence the structure of the shifted line. DuMond [5] explained more rigorously the line broadening by the effect of the initial momentum distribution of the electrons, which had not previously been taken into account. According to DuMond's explanation, monochromatic radiation, after scattering by matter at a well-defined scattering angle, suffers a change of wavelength as the result of two distinct types of process. The first of these two shifts is the result of the momentum imparted to a single target electron. This effect is known as the Compton Effect. The second effect can be understood as the result of the initial momentum of the scattering electron. This effect is known as Doppler Effect. This Effect results in a broadening of the shifted Compton line with a definite structure which is governed the momentum distribution of the scattering electron.

The relationship between the electron momenta and the line broadening was obtained, assuming a scattering process between a photon and a free but moving electron. If this assumption is to be valid for electrons bound in atoms,

molecules, and solids, the collision between the photon and the electron must be impulsive [3]. The consequence of the impulse approximation implies that the energy transfer $E_{tran\ to}$ the recoil electron must greatly exceed its binding energy E_{bind}, recoil electron will have high kinetic energy and is ejected into the continuum as a plane wave. Furthermore, during the scattering event, the excited atom cannot relax to take account of the hole left by the recoiling electron until it has completely escaped from the atom. Under this condition, the nuclear potential $V(r)$ seen by the target electron is the same immediately before and immediately after the interaction. As a result, the potential energy term V(r) will cancel out in the conservation energy equation. Thus the impulse approximation the collision occurs between a photon and an individual moving but unbound electron. Using the nomenclature of figure 1 and assuming the cancellation of the potential energy $V(r)$ terms, the conservation equation in the nonrelativistic approximation, $\hbar\omega_1 << mc^2$, can be written as:

$$\omega_1 - \omega_2 = (P_1 + K)^2 / 2m - |P_1|^2 / 2m = |K|^2/2m + K.P_1/m \quad (4)$$

Where $K = k_1 - k_2$ is the scattering vector and is conventionally chosen as the z-axis. The first term in equation (4) is the familiar Compton shift given by equation (2). The second term is linearly dependent upon one component, pz, of the electron's ground-state momentum, and hence describes the Doppler broadening of the shifted line.

Since the Compton profile $J(p_z)$ given by equation (1) is subject to the normalization rule:
$$\int J(p_z)\ dp_z = Z \quad (5)$$

Where Z is the number of electrons and since $n(p)$ is the probability density distribution of finding an electron with momentum p, then the spectral intensity of the Compton profile is proportional to the number of electrons for which equation (4) is satisfied. Therefore, the Compton profile $J(p_z)$, given by equation (1) is one-dimensional projection of 3-dimensional momentum density distribution projected on the scattering vector, K.

Compton Scattering from unbound electrons: The incoherent or Compton scattering refers to the process in which an incident photon imparts some of its energy to the scattering electron, the photon changes phase and the electron gains kinetic energy. The magnitude of the changes depends on the scattering angle and the energy of the incident photon. This is in fact the main difference with the coherent scattering.

When a photon is scattered by a free electron initially at rest to the extent that the atomic binding energy is negligible compared to the energy acquired from the photon, the kinematics for the process are derived from the usual conservation laws and the differential scattering cross-section is predicted with good accuracy by the Klein-Nishina formula [16]. For unpolarized radiation this cross-section is:

$$(d\sigma/d\Omega)_{K-N} = (1/2)r_0^2(\omega_2/\omega_1)^2(\omega_2/\omega_1 + \omega_1/\omega_2 - \sin^2\theta) \quad (6)$$

Where, r_0 is the classical electron radius, $r_0 = e^2/mc^2 = 2.8\ x\ 10^{-15}$ m, θ is the scattering angle, ω_1 and ω_2 are the incident and scattered photon energies which are related to the Compton shift formula, equation (3).

In the low energy limit where $\omega_1 = \omega_2$, Klein-Nishina cross-section is equal in magnitude to the Thomson cross-section,

$$(d\sigma/d\Omega)_{Th} = (1/2)\ r_0^2\ (1 + \cos^2\theta) \quad (7)$$

One important aspect of the Klein-Nishina cross-section given by equation (6) is that, the spatial distribution of the intensity of the scattered photons possesses rotational symmetry, with the direction of the incident ray axis, (see Fig 1).

In spite of this symmetry, the distribution is not completely isotropic. The degree of anisotropy varies strongly with the incident photon energy. At higher energies, above about 100 KeV, the photons are mostly scattered forwards, indicating a strong anisotropy. At energies around 30 KeV, the distribution tends to be more isotropic. For unpolarized radiation, there is a factor 2 in the scattering at 90^0 and 180^0. At these low energies the angular variation of the Klein-Nishina cross-section is small and the anisotropy is lost as the Klein-Nishina cross section approaches the Thomson cross- section equation (7).

Compton Scattering from bound electrons: Incoherent scattering of photons by bound electrons implies that the electron binding energy cannot be neglected. Despite its good accuracy (i.e. < 1% error), the Klein-Nishina differential cross section for a free electron is applicable as long as the electron binding energy is negligible. However, the departures from the Klein-Nishina equation (6), occurs at low photon energies because of the electron binding effects.

The decrease in the probability for incoherent scattering of photons by bound electrons over that for free electrons arises because the energy transfer to bound atomic electron is practically impossible unless the electron gains that amount of energy necessary for it to make a transition to some empty higher energy state. As the binding energy becomes large, approaching infinity, the whole atom absorbs the energy transferred. As a result, the coherent (Rayleigh) scattering probability increases. To correct the incoherent scattering cross-section for electron binding, a multiplicative factor is applied to the Klein-Nishina differential scattering cross section. The derivation of this multiplicative factor is based on the first order Born approximation.

The First Born approximation: The first Born approximation corresponds to the case where the coupling between the photon and the target electron is weak (see [17]). The frist Born approximation is based on the following assumptions: (i) the interaction between the incident photon and the target is weak. The consequence of this assumption is that scattering process is viewed as an interaction of a photon with an individual electron thus eliminating all the other effects from the scattering system. (ii) As a result of assumption (i) the incident and scattered photons can be described by plane waves (i.e. the incident photon energy must be high compared with the binding energy of the electron. In addition, the amplitude of the scattered wave is small compared with incident amplitude. Under this condition an energy transfer to the scattering electron is assured. As a result of the first Born approximation, the differential scattering cross-section is given as:

$$(d\sigma/d\Omega) = (d\sigma/d\Omega)_{k-N}S(K,\omega) \quad (8)$$

The multiplicative scattering factor $S(K,\omega)$ is a function of both the momentum transfer $K = k_1 - k_2$ and the energy transfer $\omega = \omega_1 - \omega_2$. The general behavior of $S(K,\omega)$ is that it approaches zero or unity depending on whether the momentum and energy transfer to the atomic electron is small or large, respectively, compared to the initial electron energy and

momentum. Thus $S(K,\omega)$ represents the probability that an atom will absorb energy and be raised to an excited or ionized state when an incident photon transfers momentum and energy to any of the atomic electrons. This probability enables $S(K,\omega)$ to be expresses using the Golden Rule as,

$$S(K,\omega) = \omega_2/\omega_1 \, \Sigma_f \, \Sigma_i \, | <f | \, \Sigma_j \, \exp \, i(K\cdot r_j) \, | \, I > |^2 \, \delta \, (E_2 - E_1 - \omega) \quad (9)$$

The delta function ensures conservation of energy during the scattering process. $| i>$ and $<f |$ are the initial and final electron states. The matrix element describes the scattering amplitude and the factor $\Sigma_j \, \exp \, i(K\cdot r_j)$ which is the Born operator is the phase of the scattering amplitude from the jth electron. Substituting for $S(K,\omega)$ in equation (8) gives the following general non-relativistic scattering formula,

$$(d^2\sigma/d\Omega d\omega) = (d\sigma/d\Omega)_{k\text{-}N} \, \omega_2/\omega_1 \, \Sigma_f \, \Sigma_i \, | <f | \, \Sigma_j \, \exp \, i(K\cdot r_j) \, | \, i > |^2 \, \delta \, (E_2 - E_1 - \omega) \quad (10)$$

The Compton profile for moving bound electrons can now be derived after one further approximation. The following section shows how the Compton profile $J(p_z)$ given by equation (1) and subjected to the normalization condition, equation (5) can be extracted from the spectral distribution given by equation (10). This is done within the framework of the Impulse Approximation (IA).

The Impulse approximation: The central feature of the IA is the effective removal of the potential energy terms from the energy conservation law. To arrive at this important result, it is essential to emphasize the assumption underlying this approximation. In the IA it is assumed that: (1) the time the photon spends probing the electron distribution $(\Delta t = \hbar/\Delta\omega)$, where $\Delta\omega$ is the energy transfer. (2) the energy transfer is much larger than the one-electron binding energies, $\omega >> E_{bind}$.

For the interaction to be impulsive, the duration must be very short. This implies that the energy transfer must be very large provided that it is within the limit of assumption (2). Under this condition, the interaction is viewed as taking place between a photon and an individual electron. The recoiling electron must be emitted so quickly that it has completely left the system before the other electrons can relax, to take account of the positive hole produced. For this to occur, the energy transfer to the electron must greatly exceed the one-electron binding energies, in accord with assumption (2).

Therefore, the consequence of the IA is that, for a short duration, the potential $V(r)$ that the electron is moving in may be thought of as a constant. Thus it cancels out in the energy conservation equation. The energy conservation expressed by the delta function in equation (9) or (10) is the same as the one given by equation (4). i.e.

$$\omega = |K|^2/2m + K\cdot P_1/m \quad (11)$$

The delta function states that the scattered photon is shifted in frequency both by the momentum transfer term $(K^2/2m)$ and the Doppler shift component $(K\cdot P_1/m)$. For a particular scattering angle θ, the scattering vector K and p_z are fixed and the summation for each value of ω is over all states in the p_x, p_y plane. For $| K |^2 >> | P_1|^2$, where P_1 is the initial electron momentum, the IA allows the final electron state to be written as a continuum plane wave, $\exp \, (ip_2\cdot r_j)$. The matrix element of equation (10) can be rewritten as,

$$\Sigma_j \, | \, \int \Psi_i \, (r_j) \, \exp \, [i(K - p_2) \cdot r_j \,] \, dr_j |^2$$

Since the conservation of momentum implies that, $P_2 = K + P_1$, the matrix element above reduces to $\Sigma_j \, |\chi_i \, (p_j)|^2$ the one electron momentum density distribution where $\chi_i \, (p_j)$ is the Fourier transform of $\Psi_i \, (r_j)$. The function $\Sigma_j \, |\chi_i \, (p_j)|^2$ gives the probability of finding the initial electron with a given momentum P_j. The cross-section given by equation (10) can now be rewritten as,

$$(d^2\sigma/d\Omega d\omega)=(d\sigma/d\Omega)_{k\text{-}N}(\omega_2/\omega_1)(m/|K|)\int\!\int n(p_x,p_y,p_z)dp_x dp_y \quad (12)$$

It has been shown based on the IA, that the Compton profile of equation (1) can be extracted from the spectral distribution. The transformation from energy to momentum scales being accomplished by the equation,

$$P_z/mc = \frac{\omega_1\omega_2(1-\cos\theta)/mc^2 - (\omega_1-\omega_2)}{(\omega_1{}^2 \omega_2{}^2 - 2\omega_1\omega_2 \cos\theta)^{1/2}} \quad (13)$$

The need to measure the electron momentum distribution rather than the more usual position distribution commonly associated with x-ray diffraction studies is very well justified. Since electrons in real materials are in motion, it is more informative to view the dynamics of such systems in momentum instead of position space. Another important aspect of measuring a momentum distribution is the fact that both momentum and position are related via the Dirac-Fourier transform. The significance of such a transform makes the Compton profile particularly sensitive to the behavior of the slower moving outer electrons, in particular those responsible for the interatomic effects which lead to the formation of solids and molecules and therefore can be used to test their quantum mechanical description (see figure 3).
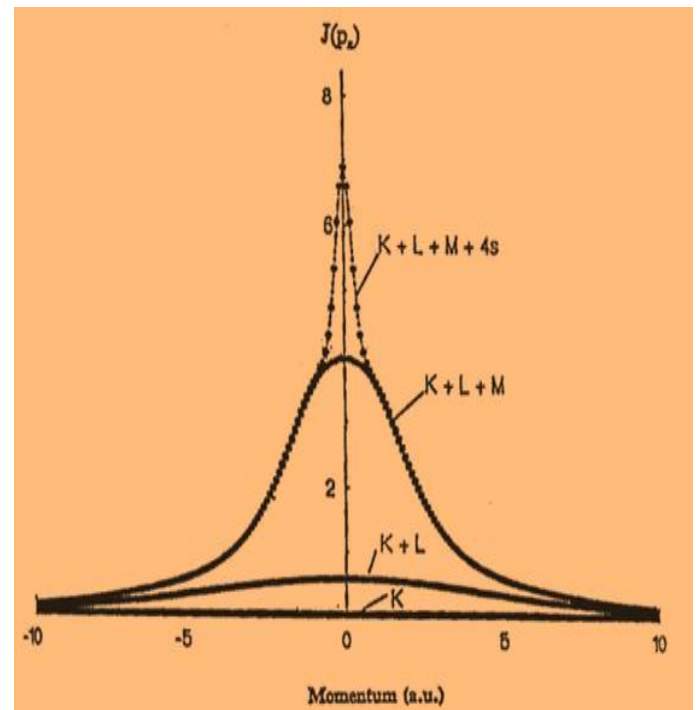

Figure 3: The free atom Compton profile of nickel calculated numerically from [23]. The contributions from the individual electron shells are also shown.

Over the range of energies below 1MeV, the Compton cross-

section is proportional to the atomic number Z whereas the photoelectric cross-section is approximately proportional to Z^4/ω_1^3 where ω_1 is the incident photon energy. This implies that the ratio of Compton to photoelectric cross section is approximately proportional to ω_1^3/Z^3 (see figure 4).
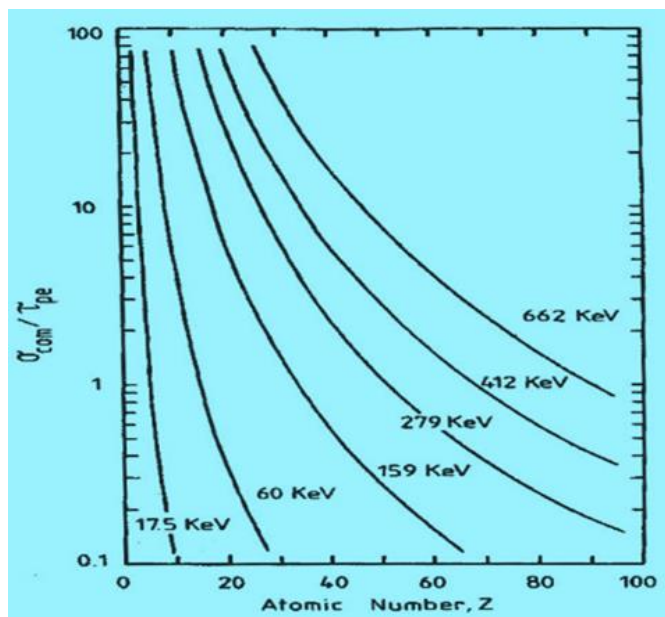

Figure 4: Ratio of the energy transfer to the K-electron binding energy in Compton scattering at 150^0 scattering angle plotted as a function of atomic number Z of the scatterer [7].

For 662 keV gamma ray radiation, the Compton cross section is greater than the photoelectric cross section up to about Z=90 [18-23]. For example, if Compton profile measurement is to be carried out using x-ray energy of 15 keV compared to gamma ray energy of 662 keV, the gamma ray experiment will gain a factor of about 10^5 in time for the same sample and the same source strength. As a result, the higher energy of the gamma ray makes Compton profile measurements to be performed on a wide range of high Z-materials and their alloys which are completely impractical at the present x-ray energies.

3. Results:

Experimental Requirements: Since the intensity profile of Compton scattered x-rays or gamma rays is a measure of the electron momentum distribution in a scatterer and a sensitive probe of its electronic structure, precise measurements of Compton profiles require three important parameters:

(1) High statistical accuracy. This requirement is based on the fact that, low statistical accuracy of measurements implies that information contained in the Compton profile will be hidden by the large statistical error. This in turn prevents precise measurements of the electron momentum distribution in a scatterer. However, high statistical accuracy in Compton profile measurements can generally be realised by either increases in the count rate of x-rays or γ-rays, which depends on the intensity and energy of the incident photons as well as the scatterer to be studied, or using detection systems which possess high efficiency at the energy range of interest.

(2) High momentum resolution. This requirement is based on the fact that, a quantitative discussion of the electronic structure of metals and alloys as to the discontinuity at Fermi momentum and fine structures in the region below it, requires high momentum resolution. Therefore, a low momentum resolution is expected to smooth out detailed fine structure in the shape of the Compton profile. In principle, high momentum resolution Compton profile measurements can be achieved using high monochromatic incident photons, high resolution of the scattered photons by means of a small divergence of the scattering angle, and detection systems which possess high energy resolution in the energy range of interest. However, it is important to emphasise the fact that, in practice, the conditions of the latter requirement often conflict with the former requirement. In normal experimental conditions the choice of one of the above requirements will depend on the type of measurement to be made. But in actual Compton profile measurements, it is a general practice as to find the best compromise between the requirements of high resolution and high statistical accuracy.

(3) High signal-to-noise ratio. This last requirement is based on the fact that, a poor signal-to-noise ratio will affect the Compton profile in two ways: (i) the data will contain noise and therefore negatively reflects its quality; (ii) background subtraction will be unreliable at larger values of electron momentum as the signal-to-noise ratio drops to 1:1. This will also affect normalisation. However, high signal-to-noise ratio can be achieved using an effective radiation shielding for the detector and the experimental set-up should be constructed in such a way that a reliable independent background measurement can be carried out.

Energy Limitations: Perhaps the most important single factor in the Compton scattering technique is the choice of the radiation source with regard to its energy and intensity. In fact, this choice will have a great effect on specifying the scatterers to be studied and the overall design of the experimental set-up. The selection of the appropriate photon energy in studying a typical scatterer by means of Compton scattering techniques is influenced by the requirement of the impulse approximation (see [7]), and practical consideration of intensity. The validity of the impulse approximation requires that the energy transfer to the electron in a Compton scattering event be large compared to the electron binding energy. To ensure the validity of the impulse approximation, Compton profile measurements have been limited to low Z-materials at low photon energies and the extension to high photon energies has permitted measurements to high Z- materials.

A typical x-ray Compton scattering spectrometer involves an x-ray tube with a Mo target; soller slits collimators, analysing crystal and scintillation counter. The incident x-ray beam is collimated using source Soller slits. The inelastically scattered beam through a fixed angle is analysed using Bragg spectrometer and detected by a NaI scintillation counter. The most common x-rays tubes radiation used for Compton profile measurements are the characteristic **K** x-rays of Mo (17 KeV), Ag (22.2 KeV) and W(60 KeV).

A typical gamma ray Compton spectrometer is made up of a Compton source placed in a lead block, an evacuated scattering chamber, and a detector. The practical considerations of intensity, resolution and background dictate a scattering geometry with a scattering angle as high as possible, being consistent with adequate shielding around the source and no parts of the scattering chamber illuminated by the source except the sample are seen by the detector. The counts are amplified, converted to a digital format (ADC), and recorded as a function of energy in a multichannel analyser (MCA). The most commonly used gamma-ray sources for Compton scattering

measurements are: 241-Am source (half-life of 458 years).With a principle transition line at 59.54 KeV and a much less intense line at 26.36 KeV. The 198-Au source (half-life of only 2.7 days), has a primary line at 412 KeV and is produced by a small strip of gold foil activated by neutron capture on 197-Au. The 137-Cs source (half-life of 30 years) is a fission product that is available at moderate cost and which has a single transition line at 661.62 KeV.

However, before the data can be interpreted, a series of energy dependent corrections have to be applied [24]. In this paper an outline of the data corrections is presented and the background, detector response function, geometrical broadening and source broadening function corrections are discussed. The order of data corrections is illustrated schematically in figure 5. The order of data corrections is illustrated schematically in figure 5.
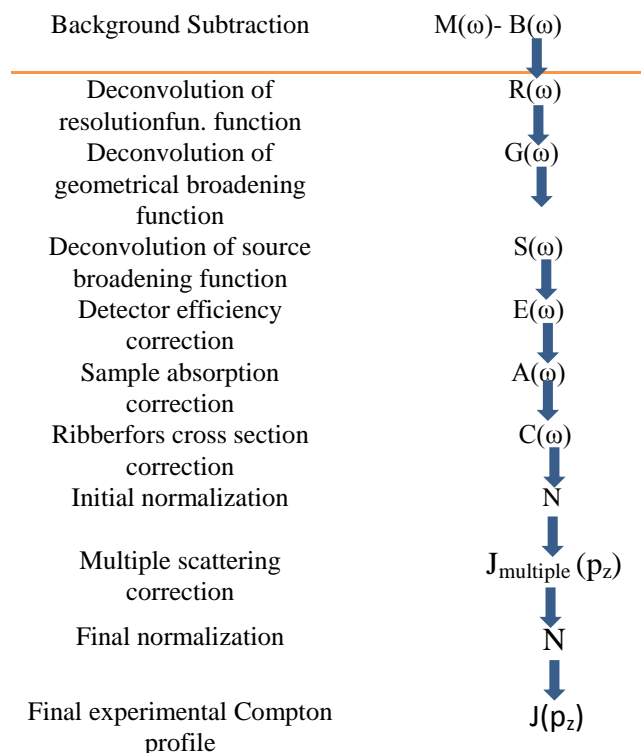
Background Subtraction	$M(\omega) - B(\omega)$
Deconvolution of resolutionfun. function	$R(\omega)$
Deconvolution of geometrical broadening function	$G(\omega)$
Deconvolution of source broadening function	$S(\omega)$
Detector efficiency correction	$E(\omega)$
Sample absorption correction	$A(\omega)$
Ribberfors cross section correction	$C(\omega)$
Initial normalization	N
Multiple scattering correction	$J_{multiple}(p_z)$
Final normalization	N
Final experimental Compton profile	$J(p_z)$

Figure5. Flow chart of the data reduction procedure used to extract the Compton profile $J(p_z)$ from the measured energy spectrum, $M(\omega)$.

Figure 6 shows the difference between the APW calculation of [30], and the experimental Compton profile of tungsten. The experimental profile was convoluted with 0.60 a.u. to mimic the experimental resolution and normalized to the same area. (1a.u. of momentum is 2.0×10^{-24} kg m s^{-1}). As can be seen from figure 6 there is a significant difference between the APW calculation and the experimental result. The most obvious feature of this comparison is the excess of electron momentum density for the APW calculation at low momenta ($p_z < 1$ a.u.). The difference between the APW calculation and the experimental profile amounts to 7.3% at J(0). On the other hand the APW calculation appears to underestimate the electron momentum density at the intermediate momenta (1.0 a.u. < p_z < 3 a.u.). However, above 3 a.u. the APW calculation is in good agreement with experiment.
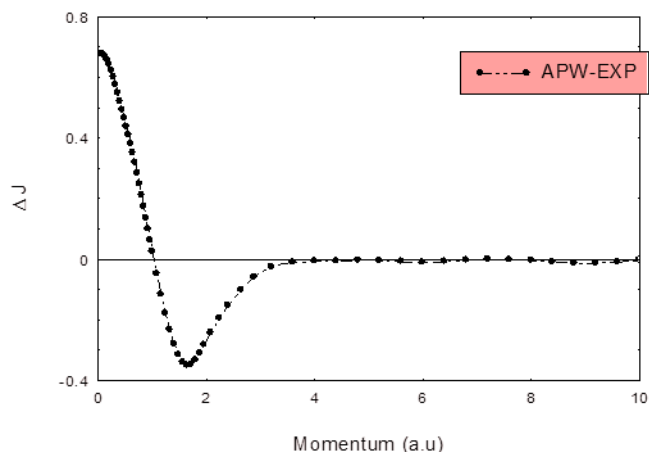

Figure 6: The difference between the APW theory and experimental Compton profile of tungsten measured with 662 KeV radiations

The discrepancies between APW calculation and experiment were attributed to some non-local exchange-correlation effects and the spin-orbital interaction effect. All these effects were neglected in the APW calculation of [30]. The non-local exchange-correlation effects which are not included in the local density approximation may affect the electron momentum distribution since the delocalization of the d electrons was shown to increase from V to Ta (see [31]). The spin-orbital interaction has been investigated through the Hamiltonian of H=ξl.s. by [32] and found that the coupling constant ξ to increase with the mass of the element and the average splitting of the d state. This implies that a correction of the spin-orbital interaction for Compton profile may appear larger with an increase of the mass of the element. This may well be applied to the case of tungsten. In a recent work on tungsten, [33], have suggested that the spin-orbital coupling may affect the Fermi surface and hence the electron momentum distribution. All these effects were neglected in the APW calculation of [30]. Therefore, the non-local exchange effect and the spin-orbital interaction correction are necessary to correct the band structure theory to bring it closer to experiment

The problem of bremsstrahlung background (BB) in association with Compton profile measurement was based on an interpretation that photoelectrons and Compton recoil electrons may introduce an extra background as the consequence of the rapid deceleration of an electron in the electric field of an atom in the target. This BB, could extend to the energy region of Compton spectrum. Because these electrons have high kinetic energy, another concern was raised that they may reach the detector and affects the measurement. This problem has been raised by [34] that the discrepancy between their experiment and theory was attributed to bremsstrahlung radiation. Calculations of photoelectron bremsstrahlung to Compton scattering cross section ratios were (by the author) extended to a wide range of atomic number (up to Z=92)[35]. This is shown in figure 7. It can be seen from the figure7 that the photoelectron bremsstrahlung to Compton cross section ratios are less than 0.03% for atomic number up to Z=92.These calculations have shown that the bremsstrahlung contribution to Compton spectra is very insignificant and the discrepancies between [34] experiment and theory were not

attributed to bremsstrahlung radiation but was found (by the author) to be due to errors in data analysis.
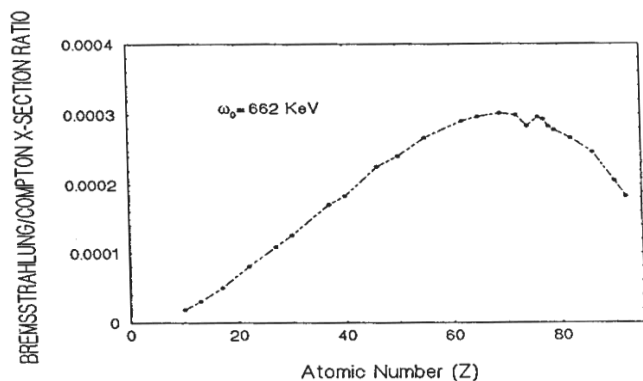

Figure 7: Bremsstrahlung to Compton cross section ratios as a function of atomic number Z for an incident photon of energy 662 KeV [34].

Since 1970 Compton profile measurements have become more frequent and the experimental results for many Z-elements reported in the literature [25-29] have been quoted to an accuracy of better than 1% for the total profiles and about 1/4 % for anisotropy measurements. This experimental accuracy has mainly been achieved from the use of γ-ray sources in conjunction with solid state detectors (SSDs) and multi-channel analyzers required to detect and record the Compton scattered energy spectra and is expected to improve further when SSDs of high resolution and efficiency become available.

4. Discussion and Conclusions:

Compton scattering is a technique for determining the momentum distribution of electrons in condensed matter. The objective of this paper is to present the Compton scattering theory to researchers generally unfamiliar with this phenomenon and to lead the researchers to understanding of the fundamental principles of the Compton Scattering Theory. The main primary purpose of this paper is to show how the Compton profile J (p_z) given by equation (1) can be extracted from the measured double scattering cross-section, following the explanation of the Compton effect and the consequent development of the Compton scattering theory which have led to an interpretation of the experimental results in terms of the electronic wave functions of the scattering system. Despite the reasonable resolution of the present gamma-ray Compton spectrometers, comparison between experimental data and the theoretical model can be made and the discrepancies can be revealed and distinguished.

Today the Compton scattering is acknowledged as an important technique for investing the electronic structure of materials; it provides a sensitive test for the accuracy of the resulting electron wave functions obtained from different theoretical models. This has been demonstrated in view of the Compton scattering experiments successfully performed over a wide range of incident photon energies (10 - 662 KeV) used in various Compton spectrometer systems distributed around the world.

Acknowledgement:

References:

[1] Compton, A. H., (1923), "A Quantum Theory of the Scattering of X-rays by Light Elements", Phys. Rev., **21**, 483

[2] Compton, A. H., (1923), "The Spectrum of Scattered X-Rays", Phys. Rev., **22**, 409

[3] Cooper, M. J., (1985), "Compton scattering and electron momentum determination", Rep. Prog. Phys., **48**,415

[4] Williams, B., (editor) (1977), "**Compton Scattering**"., New York: McGraw-Hill.

[5] DuMond, J. W. M., (1929), "**Compton Modified Line Structure and its Relation to the Electron Theory of Solid Bodies**", Phys. Rev., 33, 643

[6] Platzman, P. M. and Tzoar, N., (1965), "X-Ray Scattering from an Electron Gas" Phys. Rev., 139, 410

[7] Eiesenberger, P. and Platzman, P. M., (1970), "Compton **Scattering of x-ray from Bound Electrons**", Phys. Rev., A2, 415

[8] Cooper, M. J. and leake, J. A. and Weiss, R. J., (1965), "The. Compton Profile of Lithium",Phil. Mag. **12**, 797

[9] Cooper, M. J. and leake, J. A., (1967), The Compton profiles of graphite and diamond", Phil. Mag. **15**, 1201

[10] Cooper, M. J., and Williams, B. G., (1968), "The Compton profile of nitrogen" Phil. Mag. **22,**177**,** 543

[11] Phillips, W., and Weiss, R. J. (1968), "X-Ray Determination of Electron Momenta in Li, Be, B, Na, Mg, Al, and LiF", Phys. Rev., **171**, 790

[12] Stewart, R. A., (1975), The Compton effect- Turning Point In Physics, Science History Publications, New York

[13] Evans, R. D., (1955), **the Atomic Nucleus**, McGraw- Hill, New York.

[14] Gottfried, K., (1966**), Quantum Mechanics**. Vol. I , P5, W. A. Benjamin, Inc. New York.

[15] Jauncey, C. E. M., (1925), "Quantum Theory of the Unmodified Spectrum Line in the Compton Effect", Phys. Rev., 25, 723

[16] Klein, O. and Nishina, Y., (1994), "On the Scattering of Radiation by Free Electrons According to Dirac's New Relativistic Quantum Dynamics", The Oskar Klein Memorial Lectures (Vol 2). Edited by EKSPONG G. Published by World Scientific Publishing Co. Pte. Ltd.. ISBN #9789814335911, pp. 113-129 http://adsabs.harvard.edu/abs/1994okml.book..113K

[17] Frauenfelder, H., and Henley, E., (1974), **Subatomic Physics**, Prentice-Hall, Inc., Englewood Cliffs, New Jersey.

[18] J. L. DuBard., (1978), "Compton profile measurements of aluminum and iron with 662 KeV γ-radiation", Phil. Mag., **B37**, 273-283

[19] S. A. Hamouda; (2016), "Gamma-Ray Compton Spectroscopy of Tungsten Using 662 KeV Gamma-Ray Radiation", Journal Mordovia University Bulletin. **Vol. 26, no. 2**, 211

[20] S. A. Hamouda., (2006),"Compton Scattering Theory" Scientific Magazine Issued by Renewable Energies and

water Desalination Research Center, Tajoura, Tripoli, **Vol. 6/ No. 8**, 36

[21] S. A. Hamouda., "The influence of the Detector Response Function of Gamma-Ray Spectrometer on the asymmetry of Compton Profiles". AL – NAWAH ‚Scientific Magazine Issued by Nuclear Research Center. Tripoli- Libya **Vol 7 / No. 11** (2008)66

[22] S. A. Hamouda., (2010), "Geometrical and Source Broadening Corrections for High Gamma-Ray Compton Spectrometer**" AL** – NAWAH, Scientific Magazine Issued by Nuclear Research Center. Tripoli- Libya, Vol**.** 9 / **No** 13, 48

[23] Biggs, F., Mendelsohn, L. B. and Mann, J. B., (1975), **Atomic Data and Nuclear** Data Tables, **16**, 201

[24] S. A. Hamouda., (2016), "DATA ANALYSIS IN GAMMA-RAY COMPTON SPECTROSCOPY", MORDOVIA UNIVERSITY BULLETIN, Vol. 26, no. 2. 149

[25] Rollason, A. J., Felsteiner, J., Bauer, G. E. W., and Schneider, J. R., (1987), "Self-scattering in gamma ray sources used in Compton scattering experiments", Nucl. Instr and Meth. A256, 532.

[26] S. A. Hamouda., (2005),"Detector Efficiency Correction for High Energy γ-ray Compton Scattering Studies", Journal of Sciences Garyounis University., Second Symposium., pp236

[27] J. Felsteiner and P. Pattison, (1980), "A semi-empirical method to correct for multiple scattering effects in Compton profile measurements"**,** Nucl. Instr.and Meth. **173**, 323

[28] W. A. Reed; P. Eisenberger; K. C. Pandey and L. C. Snyder., (1974), "Electron momentum distributions in graphite and diamond and carbon-carbon bonding" Phys. Rev. **B10**, 1507

[29] S. A. Hamouda., (2010), "Multiple Scattering Correction for High Gamma-Ray Compton Experiments" The 2nd International Conference on Science and Technology (JIPMA 2009/MATERIAUX 2009). IOP Conf. Series: Material Science and Engineering **13,** 1

[30] N. I. Papanicolaou., N. C. Bacalis., and D. A. Papaconstantopoulos., (1991), Handbook of calculated Electron Momentum Distribution, Compton Profiles and X-Ray Form Factors of Elemental Solids, CRC press, Florida.

[31] C. N .Chang., Y. M. Shu., and H. F. Liu., (1993), " The Compton profiles of tantalum", J. Phys.: Condens. Matter, **5**, 5371

[32] N. C. Bacalis., K. Blathras., P. Thomaides, and D. A. Papaconstantopoulos., (1985), " Various approximations in augmented-plane-wave calculations", Phys. Rev**., B13**, 2292

[33] G. J. Rozing., P. E. Mijnarends., and R. Benedek., (1991), "Fully relativistic Calculation of two-photon momentum distribution for positron annihilation in tungsten", Phys. Rev., **B43**, 6996

[34] Andrejczuk, A., Zukowski, E., Dobrzynski, L., and Cooper, M. J., (1993), "A spectrometer for Compton scattering studies of heavy elements and the problem of bremsstrahlung background", Nucl. Instrum. Meth., **A 337, 133**–143

[35] S. A. Hamouda., **(2009),** "Compton and Bremsstrahlung Cross Sections Ratio" AL – NAWAH, Scientific Magazine Issued by Nuclear Research Center. Tripoli- Libya **Vol 8 / No. 12,** 5